Published in final edited form as:
Stem Cells. 2010 August ; 28(8): 1424–1434. doi:10.1002/stem.464.

Sin3a Is Required by Sertoli Cells to Establish a Niche for Undifferentiated Spermatogonia, Germ Cell Tumors, and Spermatid Elongation

Christopher J. Payne[a,b], **Shannon J. Gallagher**[b], **Oded Foreman**[a], **Jan-Hermen Dannenberg**[c], **Ronald A. DePinho**[d], and **Robert E. Braun**[a]

[a]The Jackson Laboratory, Bar Harbor, Maine, USA [b]Human Molecular Genetics Program, Children's Memorial Research Center, and Department of Pediatrics, Northwestern University Feinberg School of Medicine, Chicago, Illinois, USA [c]Division of Molecular Genetics, Netherlands Cancer Institute, Amsterdam, The Netherlands [d]Belfer Institute for Applied Cancer Science, Departments of Medical Oncology, Medicine, and Genetics, Dana Farber Cancer Institute, Harvard Medical School, Boston, Massachusetts, USA

Abstract

Microenvironments support the maintenance of stem cells and the growth of tumors through largely unknown mechanisms. While cell-autonomous chromatin modifications have emerged as important determinants for self-renewal and differentiation of stem cells, a role for non-cell autonomous epigenetic contributions is not well established. Here, we genetically ablated the chromatin modifier *Sin3a* in fetal Sertoli cells, which partly comprise the niche for male germline stem cells, and investigated its impact on spermatogenic cell fate and teratoma formation *in vivo*. Sertoli cell-specific *Sin3a* deletion resulted in the formation of few undifferentiated spermatogonia after birth while initially maintaining spermatogenic differentiation. Stem cell-associated markers *Plzf*, *Gfra1*, and *Oct4* were downregulated in the mutant fetal gonad, while Sertoli cell markers *Steel* and *Gdnf*, which support germ cells, were not diminished. Following birth, markers of differentiating spermatogonia, *Kit* and *Sohlh2*, exhibited normal levels, but chemokine signaling molecules CXCL12/SDF1 and CXCR4, expressed in Sertoli cells and germ cells, respectively, were not detected. In the juvenile, mutant testes exhibited a progressive loss of differentiating spermatogonia and a block in spermatid elongation, followed by extensive germ cell degeneration. Sertoli cell-specific *Sin3a* deletion also suppressed teratoma formation by fetal germ cells in an *in vivo* transplantation assay. We conclude that the epigenome of Sertoli cells influences the establishment of a niche for germline stem cells, as well as for tumor initiating cells.

Keywords

Germline; Stem cell niche; Sertoli cells; Germ cell tumor; Spermatogenesis

Correspondence: Christopher J. Payne, Ph.D., Human Molecular Genetics Program, Children's Memorial Research Center, and Department of Pediatrics, Northwestern University Feinberg School of Medicine, 2300 Children's Plaza, Box 211, Chicago, Illinois, 60614, USA. Telephone: 773-755-6316; Fax: 773-755-6593; c-payne@northwestern.edu.

DISCLOSURE OF POTENTIAL CONFLICTS OF INTEREST

The authors indicate no potential conflicts of interest.

Author contributions: C.J.P.: conception and design, data analysis and interpretation, collection and assembly of data, manuscript writing, financial support; S.J.G.: data analysis and interpretation, collection and assembly of data; O.F.: data analysis and interpretation, collection and assembly of data; J.-H.D.: provision of study materials; R.A.D.: provision of study materials; R.E.B.: conception and design, data analysis and interpretation, manuscript writing, financial support.

INTRODUCTION

An important aspect of stem cell and cancer biology is the influence of the microenvironment, or niche, on stem cell self-renewal and differentiation. In mammals, stem cell niches have been described for bone marrow[1], skin and hair follicles[2], intestine[3], neural cells[4], and the male germline[5]. The germline stem cell (GSC) niche in *Drosophila melanogaster* has been extensively characterized for both testis and ovary on the molecular and genetic levels, revealing the importance of multiple signaling pathways and cellular processes[6–10].

The male GSC niche in mice and humans is less defined. One component of the niche that plays a predominant role in regulating GSCs is the Sertoli cell, which maintains constant physical contact with all of the germ cells inside seminiferous tubules. The influence Sertoli cells have upon germ cells is profound. Two essential proteins that are expressed by Sertoli cells, and which ensure the survival of germ cells, are Steel (KITL) and glial cell line-derived neurotrophic factor (GDNF). Steel activates the kit receptor (KIT) on germ cell precursors (primordial germ cells, or PGCs) in the embryo, and on differentiating mitotic germ cells in the postnatal testis[11]. GDNF, meanwhile, activates two associated receptors, glial cell line-derived neurotrophic factor family receptor alpha 1 (GFRA1) and ret tyrosine kinase (RET), in germ cells[12, 13]. Male mice homozygous for mutations in either *Steel* (*Sl* locus in Sertoli cells) or *Kit* (*W* locus in germ cells), contain seminiferous tubules devoid of germ cells to varying degrees[14]. Mice heterozygous for *Gdnf* show a gradual postnatal loss of germ cells[15], and testes from newborn *Gdnf* $^{-/-}$, *Gfra1* $^{-/-}$, and *Ret* $^{-/-}$ mice, when transplanted into nude mouse recipients and allowed to develop, exhibit severe germ cell depletion by P7[16].

Ets related molecule (ERM; ETV5), another protein expressed by Sertoli cells, is a transcription factor whose downstream gene network pathways are required for GSC self-renewal[17]. Spermatogenic differentiation proceeds normally during the initial weeks after birth in *Erm* $^{-/-}$ males, followed by a gradual loss of the germinal epithelium until only Sertoli cells remain within the seminiferous tubules. This phenotype resembles the loss-of-function mutation in promyelocytic leukemia zinc finger (*Plzf; Zbtb16*), a transcriptional repressor expressed in GSCs and required for their self-renewal[18, 19]. ERM and PLZF ensure the maintenance of self-renewing GSCs within the niche, but are not required for germ cell differentiation or survival. *Erm*-mediated events within Sertoli cell nuclei provide one example of how the GSC niche is established, with additional mechanisms likely during testis development.

While the inhibition of *Steel*, *Gdnf*, and *Erm* in Sertoli cells dramatically affects germ cell fate, the loss of spermatogenic cells due to infertility or testicular cancer can impact the epigenetic state of Sertoli cells, leading to a global increase in histone H4 acetylation within Sertoli cell nuclei in these mutant testes[20]. *In vivo* exposure of mouse testes to histone deacetylase (HDAC) inhibitor trichostatin-A more significantly alters the Sertoli cell transcriptome when compared to germ cells[21]. HDAC1 expression has been observed in normal human Sertoli cells, and the HDAC1-associated nuclear corepressor protein SIN3A has been detected in the mouse Sertoli cell line TM4[22, 23]. We previously described the patterns of histone lysine methylation in undifferentiated and differentiating spermatogonia, including the two marks associated with pericentric heterochromatin and SIN3A, trimethylated H3-K9 and H4-K20[24]. We also detect these histone methylation marks in both dividing and non-dividing Sertoli cells (Payne and Braun, unpublished observations). Given the apparent sensitivity of Sertoli cells to epigenetic alterations, we wondered how the regulation of Sertoli cell chromatin during the fetal and juvenile periods of testis development influences the establishment of the GSC niche.

To examine the role of Sertoli cell chromatin modifications on germ cell fate, we generated mice lacking nuclear corepressor *Sin3a* specifically in Sertoli cells beginning in the fetal gonad. The generation of conditional knockout mice was essential, as $Sin3a^{-/-}$ embryos die between the blastocyst-stage of development and implantation[25]. Our current findings establish a critical role for Sertoli cells in supporting the formation and maintenance of undifferentiated spermatogonia, the germ cell population that encompasses GSCs.

MATERIALS AND METHODS

All experiments with animals were carried out in accordance with a protocol approved by The Jackson Laboratory Animal Care and Use Committee.

Generation of Conditional *Sin3a*-Deleted Mice

Hemizygous 129S.FVB-Tg(Amh-cre)8815Reb/J (*Amh-cre*) mice were mated with homozygous floxed 129-$Sin3a^{tmnRdp}$ ($Sin3a^{fl/fl}$) mice to generate *Amh-cre;*$Sin3a^{fl/+}$ offspring. These F_1 animals were then interbred to obtain *Amh-cre;Sin3afl/fl* males. Mice were genotyped by PCR analysis (primers and conditions are available upon request).

Histology and Immunohistochemistry

Adult (5- and 6-wk-old), juvenile (3- and 4-wk-old), and neonatal (3-day-old) testes were fixed for 12 h, 8 h, and 4 h, respectively, at 4°C in Bouin's solution, rinsed in PBS, and dehydrated for paraffin embedding. Five-micron sections were cut, samples were deparaffinized and rehydrated, and some sections were stained with hematoxylin and eosin. Other sections were prepared for immunohistochemistry, with some samples subjected to antigen retrieval by boiling in 0.01 M sodium citrate, pH 6.0, for 10 min (see Supplementary Table 1). Sections were blocked with 3% normal goat serum in PBS for 1 h at room temperature. Primary antibodies were diluted in PBS + 3% goat serum and added to the samples for overnight incubation at 4°C. Control reactions were performed by omitting primary antibodies from the incubations. Following PBS washes, samples were then incubated for 1 h in the dark at room temperature with fluorescence-conjugated secondary antibodies diluted in PBS + 3% goat serum [AlexaFluor 488-anti-Rabbit, 488-anti-Rat, 488-anti-Mouse (Invitrogen/Molecular Probes)]. Vectashield anti-fade mounting medium (Vector Laboratories) containing DAPI was applied to the samples, and sections were viewed using a Nikon E600 epifluorescence microscope. Supplementary Table 1 lists the sources and dilutions for all antibodies used in these studies. For the preabsorption of anti-SIN3A antibody (K-20; sc-994, Santa Cruz Biotechnology), blocking peptide sc-994 P (antigen mapping at the N-terminus of SIN3A) was added to the diluted antibody for 1 h prior to its application to the testis cross-sections.

Fetal (E16.5) testes were fixed for 2 h at 4°C in 10% neutral buffered formalin and processed as with the other samples. Following antigen retrieval, sections were incubated in 0.3% hydrogen peroxide in MeOH for 20 min to inhibit endogenous peroxidase activity. After primary antibody incubations, samples were incubated for 1 h at room temperature with biotin-conjugated goat anti-rabbit antibody diluted 1:500 (Invitrogen/Zymed). For these sections, tertiary antibody incubation was performed by the addition of streptavidin-HRP antibody at 1:100 dilution for 20 min. Peroxidase activity was then visualized by using a DAB substrate kit and hematoxylin counterstain following the manufacturer's instructions (Invitrogen/Zymed).

Reverse Transcription-Polymerase Chain Reaction and Quantitative Real Time RT-PCR

Embryos were dissected from female mice at E11.5, E12.5, E14.5, and E16.5; postnatal testes were dissected from P3 males. Genital ridges were isolated from the embryos, with

the E12.5, E14.5, and E16.5 testes identifiable by morphology. The heads of E11.5 embryos were subjected to genomic PCR (*Sry* genotyping) for sex determination. Genotyping was also performed to identify *Amh-cre;Sin3a*$^{+/+}$, *Amh-cre;Sin3a*$^{fl/+}$, and *Amh-cre;Sin3a*$^{fl/fl}$ embryos and pups. Total RNA was prepared from testes using the RNeasy Micro Kit (Qiagen), then reverse transcribed into cDNA using random hexamer primers (Invitrogen). To detect *cre* (*Amh-cre*) transgene expression in the embryonic testes, a 220-bp cDNA fragment was amplified by PCR using primers Cre1 (5′-TGGTTTCCCGCAGAACCTGAAG-3′) and Cre2 (5′-GAGCCTGTTTTGCACGTTCAC C-3′) under the following conditions: 94°C for 5 min, followed by 30 cycles at 94°C for 30 s, 60°C for 30 s, 72°C for 30 s, and a final extension at 72°C for 7 min. A 207-bp fragment of *Actb* was ampli ed as a control transcript using primers Actb-F70 (5′-CCAGTTCGCCATGGATGACGATAT-3′) and Actb-R277 (5′-GTCAGGATACCTCTCTTGCTCTG-3′) under the same thermocycling conditions. Products were separated on 3% agarose gels.

For real time RT-PCR, equal volumes of cDNA from control *Amh-cre;Sin3a*$^{+/+}$ and mutant *Amh-cre;Sin3a*$^{fl/fl}$ testes were added to 2x Power SYBRR® Green PCR Master Mix (Applied Biosystems) with specific oligonucleotide primer sets for the genes of interest (see Supplementary Table 2). Samples from three different animals for each genotype were run in triplicate on an Applied Biosystems 7500 Real-Time PCR System using SYBRR® Green dye for read-out and ROX™ dye as an internal reference. Each PCR reaction contained approximately 5–10 ng of cDNA, 1x Power SYBRR® Green PCR Master Mix, and 500 nM of each forward and reverse primer for the desired gene. *Actb* was used as an endogenous control. The threshold cycle (C_T), indicating the relative abundance of a particular transcript, was calculated for each reaction by the system software. Quantification of the fold change in gene expression between *Amh-cre;Sin3a*$^{fl/fl}$ samples and *Amh-cre;Sin3a*$^{+/+}$ samples was determined by using the formula $2^{-\Delta\Delta CT}$, in which $\Delta\Delta C_T = [(C_T \text{ of gene of interest} - C_T \text{ of } Actb)_A - (C_T \text{ of gene of interest} - C_T \text{ of } Actb)_B]$, where $_A$ = *Amh-cre;Sin3afl/fl* and $_B$ = *Amh-cre;Sin3a*$^{+/+}$. Fold change in transcript levels for genes expressed in *Amh-cre;Sin3a*$^{fl/fl}$ testes relative to *Amh-cre;Sin3a*$^{+/+}$ testes was plotted in $\log_2$ using Prism 5 software (GraphPad). As the values for all genes expressed in *Amh-cre;Sin3a*$^{+/+}$ testes had an arbitrary unit of 1, they were omitted from the graphs generated by the software. Values plotted are mean +/− SEM. Statistical analysis was performed using Prism 5, employing ANOVA; *p<0.05; **p<0.01; ***p<0.001.

Transplantations and Testicular Teratoma Formation

Adult (16-wk-old) wild type *Amh-cre;Sin3a*$^{+/+}$ male mice were anesthetized with tribromoethanol (250 mg/kg) injected IP, with analgesics carprofen (5 mg/kg) and buprenorphine (0.05 mg/kg) administered SQ. After the removal of fur and preparation of skin at the surgical site, a 5–8 mm incision was made between the last rib and iliac crest. Subcutaneous tissue was incised to expose the abdominal wall, and each testis was elevated sequentially through a 4–7 mm incision in the abdominal wall by placing a forceps under the posterior pole of the testis and lifting until the organ was completely outside the abdomen. A small hole was made on the testis surface using Dumont forceps, and a square flap of tunica albuginea was peeled back to expose the seminiferous tubules. Donor E12.5 testes and ovaries, isolated as genital ridges from *Amh-cre;Sin3a*$^{+/+}$ and *Amh-cre;Sin3a*$^{fl/fl}$ embryos (genotypes determined after transplantations), were inserted into the cavity using Dumont forceps or a blunt probe. The flap of tunica was returned to cover the parenchyma, and the testis was placed back to its normal position within the mouse. The incision in the abdominal wall was sutured with 5-0 absorbable suture Dexon “s” w/ce-2 needle, and the skin incision was closed using nylon black monofilament suture w/c-3 needle. Following recovery, the mice were monitored daily and housed for 4 weeks to allow teratomas to form.

To ascertain tumor formation, mice were euthanized by CO_2 asphyxiation and testes were removed. Following weight measurements and photographic documentation, testes were fixed for 12 h at 4°C in Bouin's solution, rinsed in PBS, and dehydrated for paraffin embedding. Samples were step-sectioned through the tissue to generate cross-sections at different depths of the testis. Sections were then deparaffinized, rehydrated, and stained with hematoxylin and eosin.

RESULTS

Generation of Sertoli Cell-Specific *Sin3a*-Deleted Mice

Given that both spermatogenic and Sertoli cells contain epigenetic marks of transcriptional repression associated with histone modifications[24], we anticipated a broad distribution of SIN3A expression within mouse seminiferous tubules. In adult wild type testes we detected SIN3A in both germ and somatic cells (Figure 1A, arrowheads and arrows, respectively). As expected, SIN3A immunofluorescence was nuclear, associated with chromatin, and in the case of round spermatids, was present in particularly intense foci (Figure 1A, left panel). To determine the specificity of the anti-SIN3A antibody, we preabsorbed the antibody with blocking peptide prior to use, and found that this preabsorption eliminated SIN3A immunofluorescence patterns (Supplementary Figure 1). SIN3A staining of Sertoli cell nuclei raised the possibility that SIN3A-mediated chromatin modifications in Sertoli cells might influence the development of male germ cells.

To investigate whether germ cell maintenance is affected by non-cell autonomous epigenetic events, we intercrossed anti-Müllerian hormone (*Amh*)-cre transgenic mice with floxed *Sin3a* mice to generate *Sin3a* deficiency in Sertoli cells[25, 26]. Endogenous *Amh* expression in the embryo is restricted to Sertoli cells and is first detected at E11.5, with higher expression levels observed at E12.5 and beyond[27, 28]. Similar to *Amh*, expression of the *Amh*-cre transgene was first detected in male gonads at E11.5, with expression levels increasing between E12.5 and E16.5 (Figure 1D). To evaluate Cre recombinase efficiency and specificity of expression, we examined cross-sections of E16.5 *Amh*-cre;*Sin3a*$^{fl/fl}$ testes immunostained with anti-SIN3A antibody (Figure 1B). Gonocytes, or fetal germ cells within the testis, were identified using an antibody specific to germ cell nuclear antigen 1 (GCNA1)[29]. GCNA1 expression in male germ cells begins at E11.5, persists throughout embryonic and neonatal development, and continues until the diplotene/dictyate stage of the first meiotic division. In conditional *Sin3a*-deleted fetal testes, SIN3A localized primarily to GCNA1-positive gonocyte nuclei (Figure 1B, arrowheads), with no detectable levels observed in the majority of Sertoli cell nuclei examined (3.53% ± 1.27% SIN3A-positive Sertoli cells versus 98.42% ± 1.19% SIN3A-positive gonocytes, n=1071; Supplementary Table 3 and Figure 1B, arrows). We also examined P3 *Amh*-cre;*Sin3a*$^{fl/fl}$ testis cross-sections for SIN3A-positive Sertoli cells, and find a similar low percentage (data not shown). From these data, we conclude that *Amh*-cre specifically and efficiently recombines floxed *Sin3a* in Sertoli cells within mouse seminiferous tubules.

Neonatal *Amh*-cre;*Sin3a*$^{fl/fl}$ Testes Contain Differentiating Germ Cells But Lack Undifferentiated Spermatogonia

Male and female *Amh*-cre;*Sin3a*$^{fl/fl}$ pups were born with Mendelian ratios and no external physical abnormalities were observed throughout the lifetime of the animals (data not shown). However, we wondered whether deletion of *Sin3a* from fetal Sertoli cells affected spermatogenesis. To begin evaluating the role of Sertoli cell-expressed SIN3A, we analyzed conditional *Sin3a*-deleted testes from animals at various ages between birth and 6 weeks. Testis cross-sections prepared from 3-day-old males revealed equivalent numbers of GCNA1-positive germ cells when compared to controls (Figure 1C, top panel). However,

because the GCNA1 antibody does not distinguish between undifferentiated and differentiating germ cells, we used antibodies to detect the undifferentiated spermatogonial marker PLZF, which is expressed in both the “actual” stem cells and “potential” stem cells of the GSC pool[30]. Strikingly, neonatal *Amh*-cre;*Sin3a*$^{fl/fl}$ testes contained very few PLZF-positive germ cells (Figure 1C, bottom panel). This finding supported previous observations that the neonatal germ cell population is heterogeneous[31], although the PLZF-positive cell population in the mutant was greatly diminished. When control testes were double immunostained with GCNA1 and PLZF antibodies, roughly 30% of gonocytes expressed only GCNA1 (29.21% ± 1.10% GCNA1 single-positive versus 70.79% ± 1.10% double-positive, n=92; Supplementary Table 4 and Supplementary Figure 2). In contrast, almost 98% of gonocytes in conditional *Sin3a*-deleted testes expressed only GCNA1 (97.86% ± 0.93% GCNA1 single-positive versus 2.14% ± 0.93% double-positive, n=133; Supplementary Table 4). These data suggest that gonocytes destined to become undifferentiated spermatogonia lose this potential in Sertoli cell-specific *Sin3a*-deleted males.

Juvenile Conditional *Sin3a*-Deleted Testes Exhibit a Progressive Loss of Spermatogonia and a Block in Spermatid Elongation

In 3-week-old *Amh*-cre;*Sin3a*$^{fl/fl}$ testes, seminiferous tubules exhibited a relatively normal appearance, with spermatogonia distributed along the basal lamina and pachytene spermatocytes properly localized within the adluminal compartment (Figure 2A). GCNA1 distribution in juvenile conditional *Sin3a*-deleted testes was equivalent to that observed in controls (Figure 2B). However, juvenile *Amh*-cre;*Sin3a*$^{fl/fl}$ testes lacked PLZF-positive cells, with numerous seminiferous tubules exhibiting a complete absence of undifferentiated spermatogonia, and others containing just one or two (Figure 2C). These findings are consistent with the earlier observations for 3-day-old testes.

In 4-week-old conditional *Sin3a*-deleted seminiferous tubules, the number of spermatogonia residing along the basement membrane was reduced to approximately 20% of that in controls (Figure 2D, arrowheads). Many regions along the basement membrane in *Amh-cre;Sin3a*$^{fl/fl}$ testes were devoid of germ cells (Figure 2D, small arrows), and exhibited empty spaces suggestive of where spermatogonia used to reside (Figure 2D, asterisks). As very few PLZF-positive cells were seen in conditional *Sin3a*-deleted testes at 3 weeks, we interpreted this dramatic reduction in premeiotic germ cells at 4 weeks as a lack of additional differentiating spermatogonia being formed. In the adluminal compartment, some regions of round spermatids showed increased cell separation (Figure 2D, pound signs), with abnormal-looking nuclei in many of the round spermatids.

At 5 weeks, almost no spermatogonia were detected in *Amh*-cre;*Sin3a*$^{fl/fl}$ testes (Figure 2E, arrowheads). Instead, meiotic spermatocytes could be found along the basement membrane (Figure 2E, yellow arrows) and in some cases round spermatids occupied this basal location (Figure 2E, pound sign). Also, round spermatids failed to elongate and exhibited swollen, abnormal-looking nuclei with clear zones, indicative of cell degeneration. Control seminiferous tubules nicely displayed elongated spermatids in their adlumenal compartment (Figure 2E, left panel). Thus, in addition to the block in undifferentiated spermatogonia formation in neonatal *Amh*-cre;*Sin3a*$^{fl/fl}$ testes, there is also a block in round spermatid elongation observed between 4 and 5 weeks. We were intrigued as to how this might affect the fertility of these animals.

Adult *Amh*-cre;*Sin3a*$^{fl/fl}$ Testes Are Depleted of Germ Cells

When conditional *Sin3a*-deleted mice reached 6 weeks of age, we assessed their fertility by mating *Amh*-cre;*Sin3a*$^{fl/fl}$ males and females to wild type animals. While conditional *Sin3a*-

deleted females gave birth to offspring with normal litter sizes, no pups were born to wild type females paired with *Amh*-cre;*Sin3a*$^{fl/fl}$ males, despite the formation of vaginal plugs as evidence of copulation (data not shown). Normal fertility was observed with *Amh*-cre;*Sin3a*$^{fl/+}$ males. We then isolated and examined testes from 6-week-old conditional *Sin3a*-deleted and littermate control mice. Unlike their appearance in 4- and 5-week-old *Amh*-cre;*Sin3a*$^{fl/fl}$ testes, 6-week-old conditional *Sin3a*-deleted seminiferous tubules were severely shrunken and appeared to contain only Sertoli cells (Figure 3A, right panel). The interstitial spaces also presented the appearance of hyperplasia. When cross-sections were immunostained with anti-GCNA1, few germ cells were detected in *Amh*-cre;*Sin3a*$^{fl/fl}$ testes (Figure 3B, right panel). Numerous mutant seminiferous tubules were completely devoid of germ cells, while some tubules contained limited numbers of GCNA1-positive cells that distributed in a disorganized manner (Figure 3B, arrows). Assessment of the undifferentiated spermatogonial population in adult conditional *Sin3a*-deleted testes revealed a near-total absence of PLZF-positive cells (Figure 3C, right panel). Accordingly, adult *Amh*-cre;*Sin3a*$^{fl/fl}$ testes exhibited an 85% reduction (16.97 ± 1.16 mg versus 103.20 ± 2.72 mg, n=32) in testis weight (Figures 4D and 4E). Examination of the epididymis in *Amh-cre;Sin3a*$^{fl/fl}$ males at 5 and 6 weeks of age revealed that no mature sperm were ever generated in these mutants (data not shown). Collectively, these data suggest that there is a failure to generate mature sperm from the first wave germ cells due to extensive degeneration of the seminiferous tubule architecture between 4 and 6 weeks of age, with the apparent elimination of spermatids and spermatocytes in conditional *Sin3a*-deleted testes. This near-total germ cell loss appears more rapid than could be explained by the diminished population of undifferentiated spermatogonia alone, and appears to be tied to the misregulation of genes specific to spermatid elongation. Nevertheless, the initial block within fetal *Amh*-cre;*Sin3a*$^{fl/fl}$ testes that inhibits the formation of PLZF-positive germ cells intrigued us, so we decided to explore this primary phenotype in further detail.

Levels of Stem Cell-Associated Transcripts Are Diminished in Conditional *Sin3a*-Deleted Testes

To determine whether gonocyte- and undifferentiated spermatogonia-specific markers in addition to *Plzf* were diminished in fetal and neonatal *Amh*-cre;*Sin3a*$^{fl/fl}$ testes, we performed quantitative real time RT-PCR on *Sin3a*-deleted and control samples prepared from E11.5, E14.5, E16.5, and P3 total testis extracts. In E11.5 testes, when we first detected *Amh-cre* transcripts, stem cell-associated markers *Plzf*, *Gfra1*, *Oct4*, and *Lin28* did not exhibit a significant change in expression between the conditional *Sin3a*-deleted samples and the control samples (Figure 4). By E14.5, however, all four transcripts exhibited significantly reduced levels in *Amh*-cre;*Sin3a*$^{fl/fl}$ samples. Expression of Sertoli cell gene *Cxcl12* (stromal cell-derived factor 1/SDF1), which encodes a chemokine required for PGC migration to the gonad[32, 33], was also significantly diminished, although additional Sertoli cell markers (*Steel*, *Gdnf*, *Amh*, *Erm*, *Ngf*) were not measurably altered.

Examination of E16.5 testes revealed a further reduction in expression levels of stem cell-associated transcripts, as well as for *Cxcl12* and *Cxcr4*, which encodes a receptor for CXCL12 on germ cells, in conditional *Sin3a*-deleted samples compared to controls (Figure 4). Sertoli cell expression of *Gdnf* was significantly upregulated, and levels of both *Steel* and *Erm* were elevated. No significant decrease was observed for *Kit* and *Sohlh2*, markers for differentiating spermatogonia in the postnatal gonad[34]. In P3 testes, expression of stem cell-associated markers *Plzf*, *Gfra1*, *Oct4*, and *Lin28* was now severely diminished, and transcript levels for both *Cxcl12* and *Cxcr4* were significantly reduced (Figure 4). *Kit* and *Sohlh2* expression remained statistically unchanged, while *Gdnf* and *Erm* levels remained high. Sertoli cell expression of *Amh* and *Ngf* appeared constant throughout all timepoints. Collectively, these findings indicate that transcriptional networks downstream of *Sin3a* in

Sertoli cells are required to establish and maintain undifferentiated spermatogonia, but not to support differentiating premeiotic germ cells.

Neonatal *Amh-cre;Sin3a*$^{fl/fl}$ Testes Do Not Contain CXCL12 or CXCR4, but Exhibit the KIT Receptor and the Cytokine CSF1

Our RT-PCR data revealed the downregulation of Sertoli cell gene *Cxcl12* and the transcript for its germ cell-expressed receptor, *Cxcr4*, within fetal and neonatal *Amh*-cre;*Sin3a*$^{fl/fl}$ testes. We wanted to follow up on this result by directly examining whether the proteins encoded by these genes in conditional *Sin3a*-deleted testes could be detected by immunohistochemistry. The CXCL12-CXCR4 signaling pathway guides migratory PGCs to the newly forming gonad[32, 33] and maintains hematopoietic stem cells in their bone marrow stromal cell niche[35]. It might also serve a similar role in the postnatal testis to maintain undifferentiated spermatogonia in their appropriate microenvironment. When we examined P3 control testis cross-sections for CXCL12 and CXCR4, we confirmed the presence of CXCL12 within Sertoli cell cytoplasm and CXCR4 on spermatogonial cell surfaces (Figures 5A and 5B, left panels). Neither was detected in *Amh*-cre;*Sin3a*$^{fl/fl}$ seminiferous tubules (Figures 5A and 5B, right panels). In contrast, the KIT receptor localized to the surfaces of differentiating spermatogonia in both control and conditional *Sin3a*-deleted testes (Figure 5C). These data suggest that CXCL12 and CXCR4 may be required for the migration and maintenance of undifferentiated spermatogonia within the GSC niche, and that KIT is insufficient for this process, but utilized by differentiating spermatogonia for their survival.

Sertoli cell-expressed proteins are not the only regulators of undifferentiated spermatogonia, but are accompanied by factors that are contributed by cells of the interstitium and peritubular regions of the testis. One such factor, the cytokine colony stimulating factor 1 (CSF1), was recently identified to be expressed by peritubular myoid cells and interstitial Leydig cells, and important for spermatogonial stem cell self-renewal[36]. We therefore asked whether neonatal and juvenile *Amh*-cre;*Sin3a*$^{fl/fl}$ testes would exhibit normal CSF1 distribution. Equivalent CSF1 staining was observed in control and *Amh-cre;Sin3a*$^{fl/fl}$ samples at both ages (Figure 5D and Supplementary Figure 3). This indicates that the loss of *Sin3a* in Sertoli cells does not perturb the expression of this important niche factor contributed by Leydig cells and peritubular myoid cells.

Transplantations of Fetal *Amh-cre;Sin3a*$^{fl/fl}$ Testes Suppress the Formation of Adult Testicular Germ Cell Tumors

The results from our RT-PCR and immunohistochemistry analysis showed that the CXCL12-CXCR4 pathway is severely compromised in *Amh*-cre;*Sin3a*$^{fl/fl}$ testes. Interestingly, both CXCL12 and CXCR4 are upregulated in human testicular germ cell tumors[37]. Given that male PGCs and gonocytes can give rise to germ cell tumors in adult human testes[38], our findings suggested that the ability of *Amh*-cre;*Sin3a*$^{fl/fl}$ PGCs and gonocytes to acquire pluripotency might be impaired. Teratomas, a type of germ cell tumor containing differentiated cell types from all three germ layers[39], form spontaneously in 1–10% of inbred 129/Sv mouse testes, and have been experimentally induced by transplanting E12.5 male genital ridges into the parenchyma of adult testes[40,41]. The microenvironment of the recipient testes permits donor male PGCs to acquire pluripotency and form teratomas. Because *Amh*-cre;*Sin3a*$^{fl/fl}$ testes exhibit a significant reduction of several pluripotent stem cell-associated markers by E14.5 (*Oct4* and *Lin28*), we wondered whether transplantation of E12.5 conditional *Sin3a*-deleted testes would suppress the formation of testicular teratomas in the adult recipient mice.

Following the transplants of fetal gonads and a 4-week waiting interval, all adult testes (10/10) receiving E12.5 control testes as donor tissue formed large multilobular teratomas

(Figure 6B, top panel). Thorough examination of each of the tumors revealed multiple differentiated cell types, including cartilage, ganglion cells, and glandular epithelium, confirming teratoma formation (Figure 6B, bottom panels). In contrast, adult testes receiving E12.5 *Amh*-cre;*Sin3a*$^{fl/fl}$ donor testes had either no or greatly reduced teratoma formation relative to controls (Figure 6C, top panel). One testis was entirely free of tumorigenic tissue and another required extensive step sectioning to reveal a diminutive teratoma, comprised primarily of bone (Figure 6C, bottom panel). As expected, few adult testes (1/4) receiving E12.5 ovaries formed structures characteristic of a teratoma, with most seminiferous tubules remaining intact (Figure 6D). These recipient testes showed a thickening of the tunica albuginea with focal infiltration of small numbers of lymphocytes and macrophages. When all of the recipient testes were weighed and compared, those receiving E12.5 control donor testes exhibited a dramatically higher average value than those receiving either E12.5 *Amh*-cre;*Sin3a*$^{fl/fl}$ donor testes or E12.5 ovaries (approximately 300 mg versus < 100 mg; Figure 6E). Deletion of *Sin3a* from fetal Sertoli cells therefore suppresses the formation of testicular teratomas in transplantation assays, compromising the ability of donor PGCs and gonocytes to acquire pluripotency in an altered microenvironment.

DISCUSSION

The generation of Sertoli cell-specific *Sin3a*-deleted mice has yielded important new insights into the establishment of a niche within the mammalian testis that is able to support GSCs, a subpopulation of undifferentiated spermatogonia. Previous cell lineage tracing experiments showed that the first round of mouse spermatogenesis, which initiates shortly after birth, is derived from a population of gonocytes that do not express markers of undifferentiated spermatogonia[31]. Our finding that PLZF is expressed in only a subpopulation of neonatal GCNA1-positive gonocytes, and that this cell population is severely diminished in our *Amh-cre;Sin3a*$^{fl/fl}$ mice, suggests that it is the PLZF-positive cells that migrate to and seed the postnatal GSC niches. Stem cell-associated markers *Plzf*, *Gfra1*, *Oct4*, and *Lin28* are all downregulated in conditional *Sin3a*-deleted testes, as are Sertoli cell-expressed *Cxcl12* and germ cell-expressed *Cxcr4*. Therefore, the transcriptional network downstream of SIN3A in Sertoli cells might facilitate the formation of undifferentiated spermatogonia, but not differentiating germ cells, through a chemokine-dependent mechanism that utilizes CXCL12 and which acts upon a heterogeneous population of gonocytes. Interestingly, *Cxcl12* is also downregulated in *Erm*$^{-/-}$ mice[42]. However, as *Erm* expression does not decrease in the *Amh-cre;Sin3a*$^{fl/fl}$ testes, it suggests that *Erm* is not in the transcriptional network regulated by SIN3A. Our observation that *Plzf* and *Cxcr4* levels are coincidently diminished in *Amh-cre;Sin3a*$^{fl/fl}$ germ cells is supported by a recent study that identified a regulatory pathway in megakaryocytic cells in which the PLZF-mediated repression of a microRNA, *miR-146a*, permits the unimpeded translation of its target CXCR4[43]. Studies are currently underway to confirm whether this regulatory pathway is conserved in undifferentiated spermatogonia.

Some neonatal, juvenile, and adult *Amh-cre;Sin3a*$^{fl/fl}$ seminiferous tubules contain a PLZF-positive cell on their basement membranes, even though they represent the minority of samples. This can be explained by the tiny fraction (3.53% ± 1.27%) of SIN3A-positive Sertoli cells observed in the mutant testes at E16.5 and confirmed at P3. Thus, our cre-mediated recombination of *Sin3a* in Sertoli cells does not exhibit 100% penetrance. However, this retention of a few SIN3A-positive Sertoli cells might explain the *Amh-cre;Sin3a*$^{fl/fl}$ phenotype with respect to spermatogonial formation. Our finding that differentiating spermatogonia reside along 3-week-old mutant seminiferous tubule basement membranes suggests that these germ cells develop from the few undifferentiated spermatogonia that are present between 1-week and 2-weeks after birth. This would indicate residual stem cell activity in these PLZF-positive cells. Such activity is not sufficient to

maintain the onset of differentiation, however, as a progressive loss in differentiating spermatogonia occurs in the *Amh-cre;Sin3a*$^{fl/fl}$ testes through 5 weeks of age, when the majority of seminiferous tubules are completely devoid of spermatogonia.

The block in round spermatid elongation and the disruption of seminiferous tubule architecture observed in 4- and 5-week-old *Amh-cre;Sin3a*$^{fl/fl}$ testes are likely attributable to a mechanism that is distinct from the initial block within the fetus and neonate that inhibits undifferentiated spermatogonia formation. This would explain the absence of mature sperm in the epididymis generated from the first round of spermatogenesis. Because mislocalized round spermatids and meiotic spermatocytes in conditional *Sin3a*-deleted testes exhibit signs of cell degeneration at 5 weeks, and are then absent from seminiferous tubules at 6 weeks, this raises the likelihood that germ cells are removed from the adlumenal and basal compartments through phagocytosis. Sertoli cells exhibit phagocytic properties through the class B scavenger receptor type I on their surfaces, and readily engulf apoptotic germ cells[44]. Further analysis is required to elucidate precisely how germ cell removal is coordinated in *Amh-cre;Sin3a*$^{fl/fl}$ testes, and to identify which transcriptional networks regulated by SIN3A are implicated in the inhibition of spermatid elongation.

Interestingly, the cell degeneration observed in *Amh-cre;Sin3a*$^{fl/fl}$ testes is localized to the postnatal germ cells and not the fetal Sertoli cells. This is striking, given that deletion of *Sin3a* in cultured mouse embryonic fibroblasts causes rapid intrinsic growth arrest and increased apoptosis, adversely affecting the Myc-Mad network, the pRB-E2F pathway and p53 mediated-events[25]. The initial maintenance of spermatogenesis through 3 weeks of age in conditional *Sin3a*-deleted testes implies that Sertoli cell proliferation and survival are not impaired by the loss of *Sin3a*. Additionally, the expression of many Sertoli cell genes, including those involved in fetal and neonatal germ cell migration and proliferation (*Steel*), and adult GSC self-renewal (*Erm*) are not altered, demonstrating that Sertoli cell differentiation is surprisingly normal. Therefore, SIN3A function in fetal Sertoli cells appears to regulate transcriptional networks devoted to supporting a subpopulation of germ cells fated to become undifferentiated spermatogonia, rather than to intrinsic growth and survival.

Our finding of potential interstitial hyperplasia in 6-week-old germ cell-depleted *Amh-cre;Sin3a*$^{fl/fl}$ testes is intriguing. This putative defect could be artifactual, with the apparent increase in cell numbers due to shrinkage of the seminiferous tubule diameters. Alternatively, the hyperplasia could be real and be a result of direct loss of paracrine signaling between Sertoli cells and interstitial cells. Recent anatomical mapping of undifferentiated spermatogonia shows a correlation with their position on the seminiferous tubule basement membrane relative to regions of the interstitium containing branching blood vessels and Leydig cells[45]. It is tempting to speculate that cross-talk between Sertoli cells and interstitial cells, mediated by chromatin modifications, might establish the GSC niche beginning in the fetal gonad and continuing through the postnatal period of development. Loss of *Sin3a* from Sertoli cells does not inhibit CSF1 expression in Leydig cells or peritubular myoid cells, however, indicating that this GSC niche factor extrinsic to the seminiferous tubules is not within the regulatory network of Sertoli cell-expressed SIN3A.

The suppression of teratomas observed after fetal *Amh-cre;Sin3a*$^{fl/fl}$ testis transplantations into adult recipients demonstrates the reduced ability of these male germ cells to acquire pluripotency. Because these transplanted testes contain functional gonocytes (they go on to initiate the first round of spermatogenesis after birth), it reveals their identity to be more committed to postnatal spermatogonial differentiation than to pluripotency. It had previously been demonstrated that transplanting fetal *Steel* mutant testes generates few teratomas in adult recipient testes[39]. This result was anticipated, given that *Steel* is required for the

migration and proliferation of the entire PGC population and that *Steel* mutant testes are almost completely devoid of germ cells. Levels of *Steel* and *Kit* are not significantly altered in the conditional *Sin3a*-deleted fetal testes transplanted here, suggesting a misregulation in other signaling pathways downstream of the SIN3A corepressor.

Results generated from our current studies augment the known regulatory mechanisms underlying GSC niche establishment in model organisms[6–10]. Mammalian epigenetic chromatin modifications join the list of processes such as cell-cell adhesion and close range signaling that ensure germline maintenance through the formation of undifferentiated spermatogonia. This work underscores the importance of future studies aimed at understanding how the niche maintains stem cells and ensures proper organogenesis, with the possibility of tissue regeneration and cancer prevention as therapeutic applications.

SUMMARY

We have demonstrated that a loss of *Sin3a* in the Sertoli cells of fetal mouse testes initially maintains differentiating germ cells, but inhibits the formation of undifferentiated spermatogonia. The expression of stem cell-associated markers *Plzf*, *Gfra1*, *Oct4*, and *Lin28* is significantly decreased in fetal and neonatal *Amh-cre;Sin3a*$^{fl/fl}$ testes, while markers of differentiated spermatogonia, *Kit* and *Sohlh2*, show little change from controls. Both the KIT receptor and cytokine CSF1 distribute normally in neonatal conditional *Sin3a*-deleted testes, but the chemokine CXCL12 and its receptor CXCR4 are not detected. This suggests a possible role for the CXCL12-CXCR4 signaling pathway to maintain undifferentiated spermatogonia in their niche, regulated by the transcriptional network downstream of SIN3A in Sertoli cells. Transplanting fetal *Amh-cre;Sin3a*$^{fl/fl}$ testes into adult recipients suppresses teratoma formation, reflecting the diminished ability of these mutant male germ cells to acquire pluripotency in a new microenvironment. Collectively, these data highlight the importance of a SIN3A-regulated epigenome within the GSC niche.

Supplementary Material

Refer to Web version on PubMed Central for supplementary material.

Acknowledgments

The authors acknowledge the following grant support from the Eunice Kennedy Shriver National Institute of Child Health & Human Development, National Institutes of Health: 5K99HD055330-02 to C.J.P. and 5U54HD042454-08 to R.E.B.

The authors thank Kevin Kane, Andree Lapierre, and The Jackson Laboratory Surgical Services Staff for providing their expertise and technical skills to the testicular transplant assays. George Enders provided the gift of anti-GCNA1 antibody. C.J.P. is the recipient of an NIH Pathway-to-Independence Award from the Eunice Kennedy Shriver National Institute of Child Health & Human Development (K99/R00 HD055330). J.-H.D. is supported by grants from the Damon Runyon Cancer Research Foundation and the Dutch Cancer Society (KWF). R.A.D. is supported by the Robert A. and Renee E. Belfer Foundation. This work was supported by NIH grants to C.J.P. and R.E.B.

References

1. Schofield R. The relationship between the spleen colony-forming cell and the haemopoietic stem cell. Blood Cells. 1978; 4:7–25. [PubMed: 747780]
2. Fuchs E, Segre JA. Stem cells: a new lease on life. Cell. 2000; 100:143–155. [PubMed: 10647939]
3. Mills JC, Gordon JI. The intestinal stem cell niche: there grows the neighborhood. Proc Natl Acad Sci U S A. 2001; 98:12334–12336. [PubMed: 11675485]
4. Doetsch F. A niche for adult neural stem cells. Curr Opin Genet Dev. 2003; 13:543–550. [PubMed: 14550422]

5. Shinohara T, Orwig KE, Avarbock MR, et al. Remodeling of the postnatal mouse testis is accompanied by dramatic changes in stem cell number and niche accessibility. Proc Natl Acad Sci U S A. 2001; 98:6186–6191. [PubMed: 11371640]
6. Yamashita YM, Fuller MT, Jones DL. Signaling in stem cell niches: lessons from the Drosophila germline. J Cell Sci. 2005; 118:665–672. [PubMed: 15701923]
7. Kiger AA, Jones DL, Schulz C, et al. Stem cell self-renewal specified by JAK-STAT activation in response to a support cell cue. Science. 2001; 294:2542–2545. [PubMed: 11752574]
8. Tulina N, Matunis E. Control of stem cell self-renewal in Drosophila spermatogenesis by JAK-STAT signaling. Science. 2001; 294:2546–2549. [PubMed: 11752575]
9. Yamashita YM, Jones DL, Fuller MT. Orientation of asymmetric stem cell division by the APC tumor suppressor and centrosome. Science. 2003; 301:1547–1550. [PubMed: 12970569]
10. Li L, Xie T. Stem cell niche: structure and function. Annu Rev Cell Dev Biol. 2005; 21:605–631. [PubMed: 16212509]
11. Sette C, Dolci S, Geremia R, et al. The role of stem cell factor and of alternative c-kit gene products in the establishment, maintenance and function of germ cells. Int J Dev Biol. 2000; 44:599–608. [PubMed: 11061423]
12. Jing S, Wen D, Yu Y, et al. GDNF-induced activation of the ret protein tyrosine kinase is mediated by GDNFR-alpha, a novel receptor for GDNF. Cell. 1996; 85:1113–1124. [PubMed: 8674117]
13. Viglietto G, Dolci S, Bruni P, et al. Glial cell line-derived neutrotrophic factor and neurturin can act as paracrine growth factors stimulating DNA synthesis of Ret-expressing spermatogonia. Int J Oncol. 2000; 16:689–694. [PubMed: 10717236]
14. Tajima Y, Sawada K, Morimoto T, et al. Switching of mouse spermatogonial proliferation from the c-kit receptor-independent type to the receptor-dependent type during differentiation. J Reprod Fertil. 1994; 102:117–122. [PubMed: 7528277]
15. Meng X, Lindahl M, Hyvonen ME, et al. Regulation of cell fate decision of undifferentiated spermatogonia by GDNF. Science. 2000; 287:1489–1493. [PubMed: 10688798]
16. Naughton CK, Jain S, Strickland AM, et al. Glial cell-line derived neurotrophic factor-mediated RET signaling regulates spermatogonial stem cell fate. Biol Reprod. 2006; 74:314–321. [PubMed: 16237148]
17. Chen C, Ouyang W, Grigura V, et al. ERM is required for transcriptional control of the spermatogonial stem cell niche. Nature. 2005; 436:1030–1034. [PubMed: 16107850]
18. Buaas FW, Kirsh AL, Sharma M, et al. Plzf is required in adult male germ cells for stem cell self-renewal. Nat Genet. 2004; 36:647–652. [PubMed: 15156142]
19. Costoya JA, Hobbs RM, Barna M, et al. Essential role of Plzf in maintenance of spermatogonial stem cells. Nat Genet. 2004; 36:653–659. [PubMed: 15156143]
20. Faure AK, Pivot-Pajot C, Kerjean A, et al. Misregulation of histone acetylation in Sertoli cell-only syndrome and testicular cancer. Mol Hum Reprod. 2003; 9:757–763. [PubMed: 14614037]
21. Fenic I, Hossain HM, Sonnack V, et al. In vivo application of histone deacetylase inhibitor trichostatin-a impairs murine male meiosis. J Androl. 2008; 29:172–185. [PubMed: 18046049]
22. Lui WY, Wong EW, Guan Y, et al. Dual transcriptional control of claudin-11 via an overlapping GATA/NF-Y motif: positive regulation through the interaction of GATA, NF-YA, and CREB and negative regulation through the interaction of Smad, HDAC1, and mSin3A. J Cell Physiol. 2007; 211:638–648. [PubMed: 17226765]
23. Omisanjo OA, Biermann K, Hartmann S, et al. DNMT1 and HDAC1 gene expression in impaired spermatogenesis and testicular cancer. Histochem Cell Biol. 2007; 127:175–181. [PubMed: 16960727]
24. Payne C, Braun RE. Histone lysine trimethylation exhibits a distinct perinuclear distribution in Plzf-expressing spermatogonia. Dev Biol. 2006; 293:461–472. [PubMed: 16549060]
25. Dannenberg JH, David G, Zhong S, et al. mSin3A corepressor regulates diverse transcriptional networks governing normal and neoplastic growth and survival. Genes Dev. 2005; 19:1581–1595. [PubMed: 15998811]
26. Holdcraft RW, Braun RE. Androgen receptor function is required in Sertoli cells for the terminal differentiation of haploid spermatids. Development. 2004; 131:459–467. [PubMed: 14701682]

27. Hacker A, Capel B, Goodfellow P, et al. Expression of Sry, the mouse sex determining gene. Development. 1995; 121:1603–1614. [PubMed: 7600978]
28. Munsterberg A, Lovell-Badge R. Expression of the mouse anti-mullerian hormone gene suggests a role in both male and female sexual differentiation. Development. 1991; 113:613–624. [PubMed: 1782869]
29. Enders GC, May JJ 2nd. Developmentally regulated expression of a mouse germ cell nuclear antigen examined from embryonic day 11 to adult in male and female mice. Dev Biol. 1994; 163:331–340. [PubMed: 8200475]
30. Nakagawa T, Sharma M, Nabeshima Y, et al. Functional hierarchy and reversibility within the murine spermatogenic stem cell compartment. Science. 328:62–67. [PubMed: 20299552]
31. Yoshida S, Sukeno M, Nakagawa T, et al. The first round of mouse spermatogenesis is a distinctive program that lacks the self-renewing spermatogonia stage. Development. 2006; 133:1495–1505. [PubMed: 16540512]
32. Doitsidou M, Reichman-Fried M, Stebler J, et al. Guidance of primordial germ cell migration by the chemokine SDF-1. Cell. 2002; 111:647–659. [PubMed: 12464177]
33. Molyneaux KA, Zinszner H, Kunwar PS, et al. The chemokine SDF1/CXCL12 and its receptor CXCR4 regulate mouse germ cell migration and survival. Development. 2003; 130:4279–4286. [PubMed: 12900445]
34. Hao J, Yamamoto M, Richardson TE, et al. Sohlh2 knockout mice are male-sterile because of degeneration of differentiating type A spermatogonia. Stem Cells. 2008; 26:1587–1597. [PubMed: 18339773]
35. Sugiyama T, Kohara H, Noda M, et al. Maintenance of the hematopoietic stem cell pool by CXCL12-CXCR4 chemokine signaling in bone marrow stromal cell niches. Immunity. 2006; 25:977–988. [PubMed: 17174120]
36. Oatley JM, Oatley MJ, Avarbock MR, et al. Colony stimulating factor 1 is an extrinsic stimulator of mouse spermatogonial stem cell self-renewal. Development. 2009; 136:1191–1199. [PubMed: 19270176]
37. Gilbert DC, Chandler I, McIntyre A, et al. Clinical and biological significance of CXCL12 and CXCR4 expression in adult testes and germ cell tumours of adults and adolescents. J Pathol. 2009; 217:94–102. [PubMed: 18839394]
38. Looijenga LH, Oosterhuis JW. Pathogenesis of testicular germ cell tumours. Rev Reprod. 1999; 4:90–100. [PubMed: 10357096]
39. Stevens LC. Origin of testicular teratomas from primordial germ cells in mice. J Natl Cancer Inst. 1967; 38:549–552. [PubMed: 6025005]
40. Stevens LC. Experimental Production of Testicular Teratomas in Mice. Proc Natl Acad Sci U S A. 1964; 52:654–661. [PubMed: 14212538]
41. Stevens LC, Hummel KP. A description of spontaneous congenital testicular teratomas in strain 129 mice. J Natl Cancer Inst. 1957; 18:719–747. [PubMed: 13502692]
42. Hess RA, Cooke PS, Hofmann MC, et al. Mechanistic insights into the regulation of the spermatogonial stem cell niche. Cell Cycle. 2006; 5:1164–1170. [PubMed: 16721062]
43. Labbaye C, Spinello I, Quaranta MT, et al. A three-step pathway comprising PLZF/miR-146a/CXCR4 controls megakaryopoiesis. Nat Cell Biol. 2008; 10:788–801. [PubMed: 18568019]
44. Nakanishi Y, Shiratsuchi A. Phagocytic removal of apoptotic spermatogenic cells by Sertoli cells: mechanisms and consequences. Biol Pharm Bull. 2004; 27:13–16. [PubMed: 14709891]
45. Yoshida S, Sukeno M, Nabeshima Y. A vasculature-associated niche for undifferentiated spermatogonia in the mouse testis. Science. 2007; 317:1722–1726. [PubMed: 17823316]

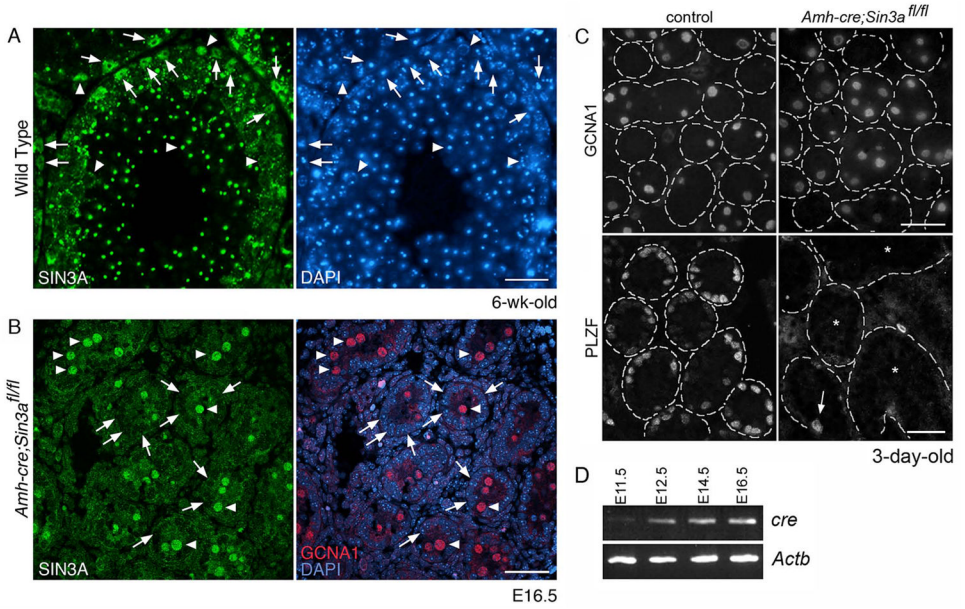

Figure 1.

Sertoli cell-specific *Sin3a*-deleted testes maintain equivalent numbers of differentiating germ cells after birth, but contain few undifferentiated spermatogonia.

(A): Cross-section of a 6-wk-old wild type testis immunostained with anti-SIN3A antibody (left) and labeled with DAPI (right). Arrows identify Sertoli cell nuclei; arrowheads denote germ cell nuclei. **(B):** Cross-section of an E16.5 *Amh-cre;Sin3a*$^{fl/fl}$ testis co-immunostained with anti-SIN3A antibody (left) and anti-germ cell nuclear antigen (GCNA; right, red), and labeled with DAPI (right, blue). Arrows identify Sertoli cell nuclei; arrowheads denote gonocyte nuclei. **(C):** Cross-sections of 3-day-old control *Amh-cre;Sin3a*$^{+/+}$ (left) and mutant *Amh-cre;Sin3a*$^{fl/fl}$ (right) testes immunostained with anti-GCNA1 antibody (top) and anti-PLZF antibody (bottom). The outlines of distinct seminiferous tubules are demarcated with dashed lines (representing basement membranes). Note the appearance of equivalent numbers of GCNA1-positive germ cells. Arrow (bottom right) identifies a single PLZF-positive spermatogonium in the field of view. Asterisks denote seminiferous tubules completely devoid of undifferentiated spermatogonia. **(D):** RT-PCR products for *cre* (*Amh-cre*) and *Actb* genes expressed in E11.5 gonads and E12.5, E14.5, and E16.5 testes. Note the increasing levels of cre that correspond with developmental progression. Scale bars represent 50μm (A), 25μm (B), 25 μm (C, top panels), and 50μm (C, bottom panels).

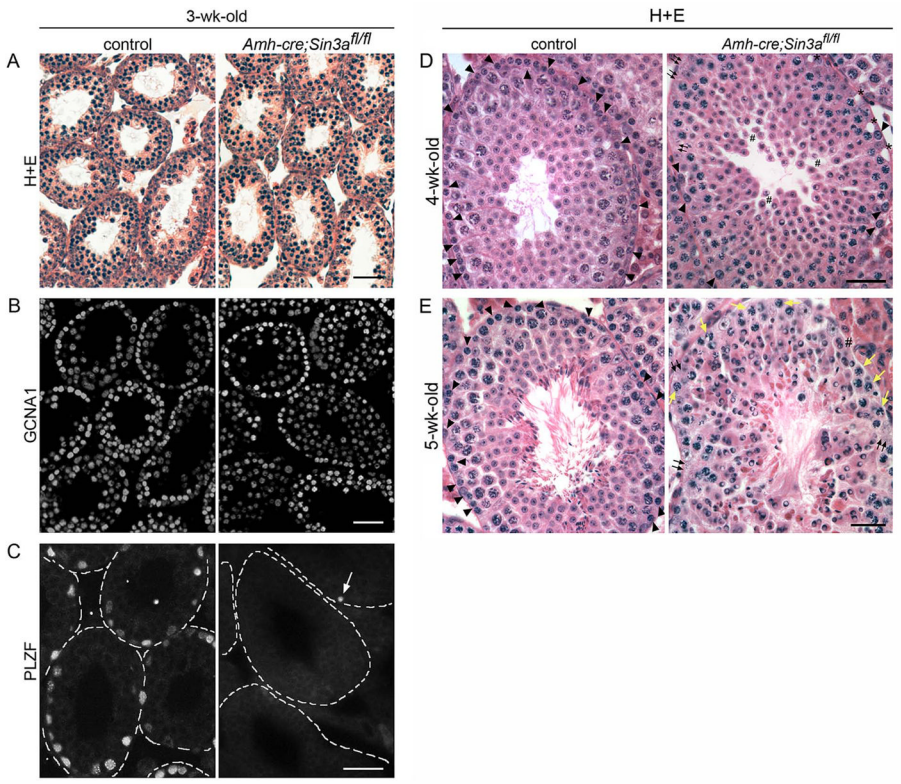

Figure 2.

Juvenile *Amh-cre;Sin3a*$^{fl/fl}$ testes exhibit a progressive loss of spermatogonia and a block in spermatid elongation.

(A): Cross-sections of 3-wk-old control *Amh-cre;Sin3a*$^{+/+}$ (left) and mutant *Amh-cre;Sin3a*$^{fl/fl}$ (right) testes stained with hematoxylin and eosin (H+E). **(B):** Cross-sections of 3-wk-old control (left) and conditional knockout (right) testes immunostained with anti-GCNA1 antibody. Note the appearance of equivalent numbers of GCNA1-positive germ cells. **(C):** Cross-sections of 3-wk-old control (left) and conditional knockout (right) testes immunostained with anti-PLZF antibody. The outlines of distinct seminiferous tubules are demarcated with dashed lines (representing basement membranes). Arrow identifies a single PLZF-positive spermatogonium in the field of view. **(D):** Cross-sections of 4-wk-old control (left) and conditional knockout (right) testes stained with H+E. Arrowheads identify spermatogonia that reside along the basement membrane; small black arrows indicate regions of the basal compartment devoid of germ cells; asterisks denote empty spaces suggestive of where spermatogonia used to reside; pound signs mark the adlumenal compartment where round spermatids exhibit increased cell separation from each other. **(E):** Cross-sections of 5-wk-old control (left) and conditional knockout (right) testes stained with H+E. Arrowheads identify spermatogonia on the basement membrane; small black arrows indicate regions devoid of germ cells; small yellow arrows denote meiotic spermatocytes that now reside along the basement membrane; pound sign marks round spermatids occupying the basal compartment. Note the absence of elongated spermatids in the *Amh-cre;Sin3a*$^{fl/fl}$ testis, and the abnormal-looking round spermatid nuclei with clear zones, indicative of cell degeneration. Scale bars represent 50μm (A–E).

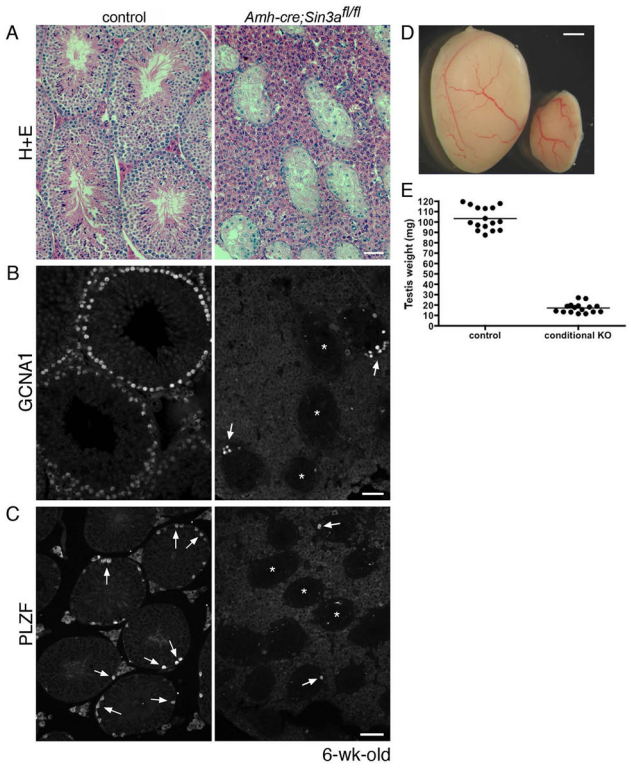

Figure 3.

Adult *Amh-cre;Sin3a*$^{fl/fl}$ testes are depleted of germ cells.

(A): Cross-sections of 6-wk-old control *Amh-cre;Sin3a*$^{+/+}$ (left) and mutant *Amh-cre;Sin3a*$^{fl/fl}$ (right) testes stained with hematoxylin and eosin. Note the reduced diameters of *Amh-cre;Sin3a*$^{fl/fl}$ seminiferous tubules. **(B):** Cross-sections of adult control (left) and conditional knockout (right) testes immunostained with anti-GCNA1 antibody. Arrows identify GCNA1-positive germ cells in two seminiferous tubules; asterisks denote three seminiferous tubules completely devoid of germ cells. **(C):** Cross-sections of adult control (left) and conditional knockout (right) testes immunostained with anti-PLZF antibody. Arrows identify PLZF-positive spermatogonia; asterisks denote three seminiferous tubules in the mutant cross-section completely devoid of undifferentiated spermatogonia. **(D):** Representative examples of 6-wk-old control *Amh-cre;Sin3a*$^{+/+}$ (left) and mutant *Amh-cre;Sin3a*$^{fl/fl}$ (right) testes. **(E):** Weights of 6-wk-old control (left) and conditional knockout (right) testes. Scale bars represent 50μm (A, B), 75μm (C), and 1mm (D).

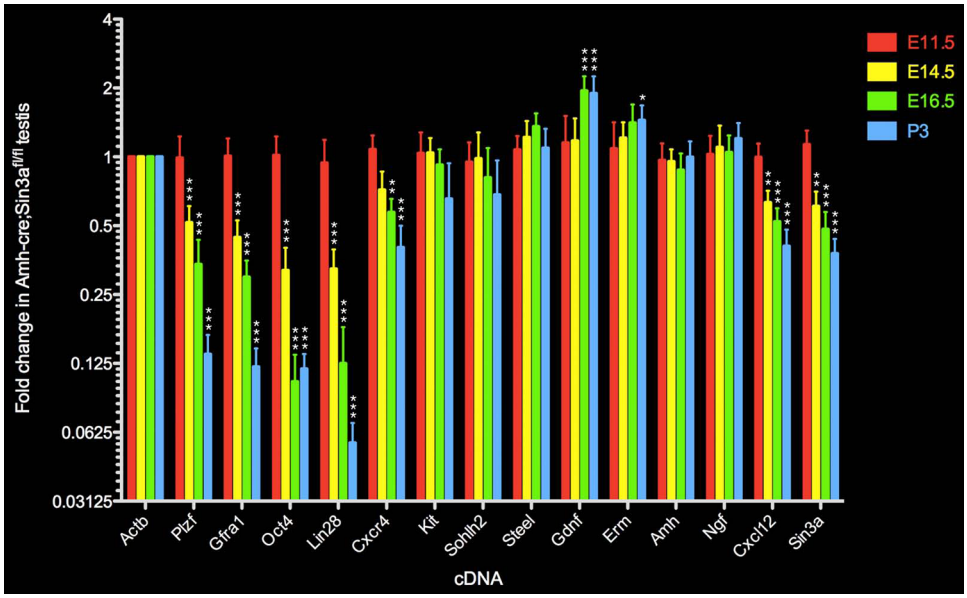

Figure 4.

Levels of transcripts specific to gonocytes and undifferentiated spermatogonia are diminished following *Sin3a* deletion in fetal Sertoli cells.

Quantitative real time RT-PCR analysis depicting the fold change in expression of selected gonocyte and undifferentiated spermatogonia-specific genes (*Plzf*, *Gfra1*, *Oct4*, *Lin28*), differentiating germ cell-specific genes (*Kit*, *Sohlh2*), Sertoli cell genes (*Steel*, *Gdnf*, *Amh*, *Cxcl12*, *Erm*, *Ngf*), germ cell gene *Cxcr4*, germline and soma gene *Sin3a*, and internal control gene *Actb* in E11.5 (red), E14.5 (yellow), E16.5 (green), and P3 (blue) mutant *Amh-cre;Sin3a*$^{fl/fl}$ testes relative to gene expression levels in control *Amh-cre;Sin3a*$^{+/+}$ testes (given an arbitrary value of 1 for all genes in control testes, not shown in this plot). Data are represented as mean values +/− SEM. Statistical comparisons with control testis-expressed genes: *p<0.05; **p<0.01; ***p<0.001.

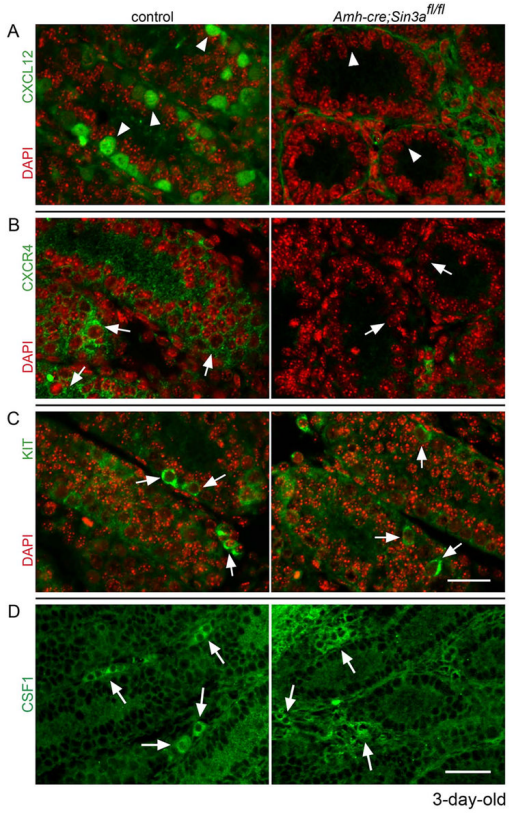

Figure 5.

Chemokine CXCL12 and its receptor CXCR4 are not detected in neonatal *Amh-cre;Sin3a*$^{fl/fl}$ testes, while the KIT receptor and cytokine CSF1 distribute normally. Cross-sections of 3-day-old control *Amh-cre;Sin3a*$^{+/+}$ (left) and mutant *Amh-cre;Sin3a*$^{fl/fl}$ (right) testes, immunostained with **(A):** anti-CXCL12 antibody (green), **(B):** anti-CXCR4 antibody (green), **(C):** anti-KIT antibody (green), **(D):** anti-CSF1 antibody (green) and labeled with DAPI (red, A–C). Arrowheads denote Sertoli cell cytoplasm and extracellular regions; arrows identify spermatogonia (A–C) and clusters of Leydig cells in the interstitium (D). Note the lack of CXCL12 and CXCR4 in the seminiferous tubules of the conditional knockout testes. Scale bars represent 25μm (A-C) and 50μm (D).

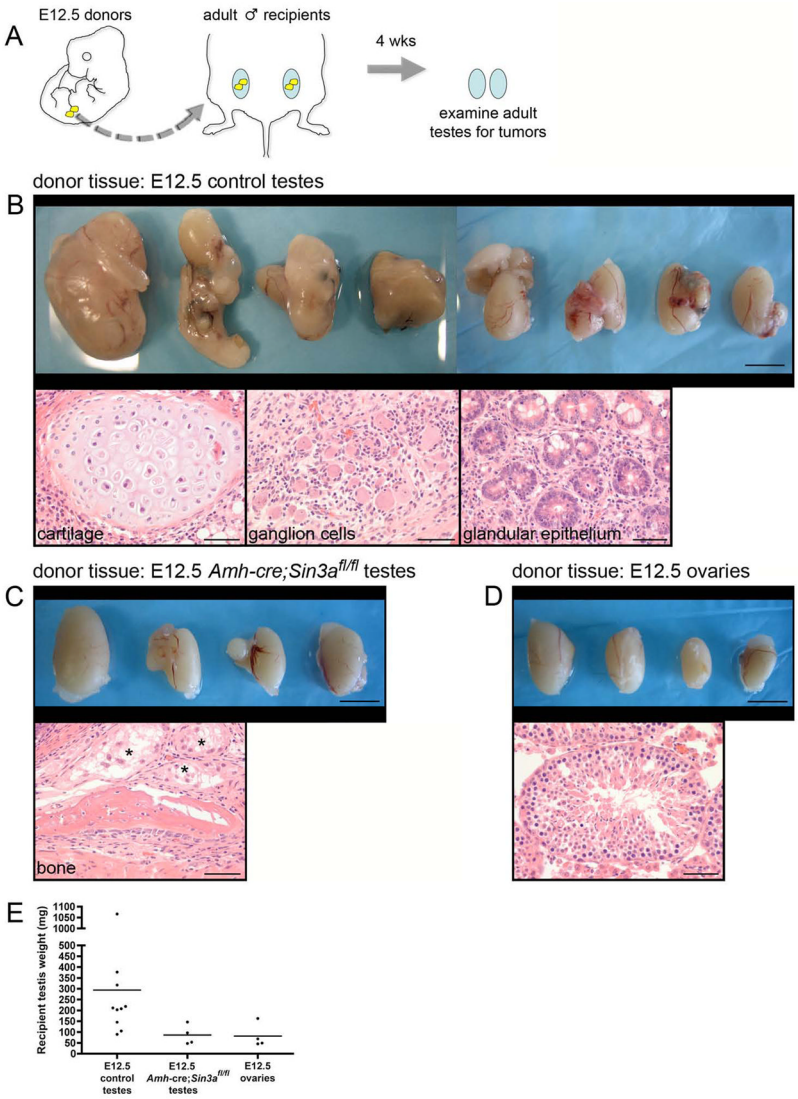

Figure 6.

Transplanted fetal *Amh-cre;Sin3a*$^{fl/fl}$ testes suppress the formation of adult testicular germ cell tumors.

(A): Schematic diagram of the transplantation assay. Gonads from E12.5 embryos (yellow) were isolated and transplanted to the testicular parenchyma of age-matched adults (blue). Four weeks later, adult testes were removed and examined for teratomas. **(B, top panel):** Adult testes that received E12.5 control testes as donor tissue. Testes are irregularly enlarged, containing multilobular tumors. **(B, bottom panels):** Tumors from all of the testes are comprised of well-differentiated tissue arising from all three embryonic germ layers (mesoderm, endoderm, neuroectoderm), consistent with teratomas. **(C, top panel):** Adult testes that received E12.5 *Amh*-cre;*Sin3a*$^{fl/fl}$ testes as donor tissue, exhibiting modest enlargement. **(C, bottom panel):** Representative example of a teratoma from one testis containing newly formed bone. Asterisks denote degenerating seminiferous tubules. **(D, top panel):** Adult testes that received E12.5 ovaries as donor tissue. **(D, bottom panel):** Seminiferous tubule containing spermatogenic cells. **(E):** Weights of adult testes that received E12.5 control testes, E12.5 *Amh*-cre;*Sin3a*$^{fl/fl}$ testes, and E12.5 ovaries as donor

tissue. Scale bars represent 5 mm in the top panels (B–D), and 50μm in the bottom panels (B–D).